Sulfates Dramatically Stabilize a Salt-Dependent Type of Glucagon Fibrils

Jesper Søndergaard Pedersen,* James M. Flink,† Dantcho Dikov,‡ and Daniel Erik Otzen*
*Department of Life Sciences, Aalborg University, Aalborg, Denmark; †Novo Nordisk A/S, Bagsværd, Denmark; and ‡Novo Nordisk A/S, Gentofte, Denmark

ABSTRACT Recent work suggests that protein fibrillation mechanisms and the structure of the resulting protein fibrils are very sensitive to environmental conditions such as temperature and ionic strength. Here we report the effect of several inorganic salts on the fibrillation of glucagon. At acidic pH, fibrillation is much less influenced by cations than anions, for which the effects follow the electroselectivity series; e.g., the effect of sulfate is ~65-fold higher than that of chloride per mole. Increased salt concentrations generally accelerate fibrillation, but result in formation of an alternate type of fibrils. Stability of these fibrils is highly affected by changes in anion concentration; the apparent melting temperature is increased by ~22°C for any 10-fold concentration increase, indicating that the fibrils cannot exist without anions. In contrast, fibrillation under alkaline conditions is more affected by cations than anions. We conclude that ions interact directly as structural ligands with glucagon fibrils where they coordinate charges and assist in formation of new fibrils. As ex vivo amyloid plaques often contain large amounts of highly sulfated organic molecules, the specific effects of sulfate ions on glucagon may have general relevance in the study of amyloidosis and other protein deposition diseases.

INTRODUCTION

The formation of amyloid fibrils has been compared to a one-dimensional crystallization process (1). However, in contrast to normal three-dimensional crystals, the one-dimensional amyloid fibrils consist of nonnative proteins in a cross-β conformation (2,3). Because the amino acid sequences of folded proteins have evolved under pressure from natural selection, they have been optimized to avoid being trapped in misfolded conformations to retain a single native conformation (4). With a few possible exceptions, e.g., Curly in *E. coli* and Pmel17 in melanocytes (5), proteins that form amyloid have not been functionally optimized to form amyloid through evolution, but rather have been under selection *not* to do so. Still, by analogy to the ''single fold dogma'' for native globular proteins (6,7), it has generally been assumed that the fibrils of amyloidogenic proteins have a single, lowest-energy, fibrillar conformation dictated by their sequence, with the only exception being the prions, which are known to form strains of fibrils in different conformations (8). Nevertheless, there are numerous reports of polymorphic protein fibrils (9,10), typically interpreted as different fibrillar packing of protofilaments (11,12). Moreover, recent evidence suggests that even subtle changes in fibrillation conditions can lead to different conformational fibril-packing motifs, observable as self-propagating fibril ''strains'' of Alzheimer's β-peptide (Aβ) (13), insulin (14), and glucagon (15). Thus the preferred conformation of amyloid fibrils may not reflect an optimal energy-minimized packing, but rather the kinetically most accessible structure under the given conditions.

The amyloid-forming propensity of amyloidogenic peptides/proteins is highly modulated by environmental factors. Solvent conditions that promote partly (un)folded structures are believed to play an important role in fibrillation (16). Salts generally speed up fibrillation of many proteins including insulin (17), β_2-microglobulin (β_2M) (18), α-synuclein (19), and S6 (20), unless the salts are at concentrations that lead to stabilization of the native protein conformation. For α-synuclein, the effects of anions at concentrations >10 mM follows the forward Hofmeister series at neutral pH and the reversed series below the isoelectric point at acidic pH (19) (e.g., ClO_4^- is the least effective anion at neutral pH and the most effective at acidic pH). Similar reversals of the series are also reported in protein crystallization (21). The Hofmeister effect is generally attributed to preferential hydration of proteins, increase of surface tension, or ordering of water molecules by salt ions (22). All these phenomena favor compact conformations, though they generally require on the order of hundred millimolar to molar concentrations of salt for significant effects. However, in many cases the effects are highly dependent on the nature of the ions even at low concentrations. For the Aβ peptide, there are clear differences between the relative potency of cations, with zinc, iron and aluminum ions being much more potent than other physiologically relevant cations (23); the nucleation of Aβ fibrils appears to be entirely dependent on trace amounts of these cations (24). In addition, the effects of anions at low concentrations can have a disproportionate effect on fibrillation. Thus for β_2M, 3 mM sulfate stimulates fibrillation to the same extent as 200 mM chloride (18). This indicates that direct electrostatic interactions between β_2M and the salts

Submitted July 21, 2005, and accepted for publication February 2, 2006.

Address reprint requests to Daniel Erik Otzen, Dept. of Life Sciences, Aalborg University, Sohngaardsholmsvej 49, DK-9000 Aalborg, Denmark. E-mail: dao@bio.aau.dk.

0006-3495/06/06/4181/14 $2.00

doi: 10.1529/biophysj.105.070912

play an important role. In addition, sulfate ions induce lateral aggregation of preformed Aβ (25) and transthyretin (TTR) (26) fibrils, indicating that sulfate ions may play an important role in fibrillation in general.

Ex vivo amyloid fibrils are almost invariably associated with highly sulfated glycosaminoglycans (GAGs) (27), and it has been suggested that GAGs interact with fibrils via their sulfate moieties (28). However, general polyanions (29,30), RNA (31), and anionic surfactants (32) have also been reported to accelerate fibrillation.

In this study we have investigated the effects of various salts on the fibrillation kinetics and fibril structures of the 29-residue peptide hormone glucagon (33). Glucagon forms amyloid fibrils at both acidic (34,35) and alkaline conditions (36), which can be followed using both intrinsic Trp and in situ Thioflavin T (ThT) fluorescence (15). We have tested the effect of increasing concentrations of various salts on the fibrillation and show that the salts affect not only the kinetics of fibrillation, but also the final structure of fibrils. Fibrils formed under acidic conditions at millimolar concentrations of sulfate are dependent on anions for stability, indicating that the anions become integrated in the fibril as structural ligands. The dramatic effect of sulfate ions may have direct bearing on the structural and mechanistic role of GAGs for fibrillation in vivo.

MATERIALS AND METHODS

Pharmaceutical-grade glucagon (>98.9% pure) was purified by Novo Nordisk A/S (Bagsværd, Denmark). Thioflavin T (T3516), obtained from Sigma-Aldrich (St. Louis, MO), was used without further purification. Ultrapure GdmCl was obtained from Invitrogen (Carlsbad, CA), Glycine, HCl, and NaCl were obtained from AppliChem GmbH (Darmstadt, Germany) and >99% pure sodium sulfate was purchased from Merck (Darmstadt, Germany). Glucagon concentration was measured using the calculated extinction coefficient E (280 nm, 1 cm, 1 g/l, 6 M GdmCl, pH 6.5) = 2.369. ThT concentration was measured using an extinction coefficient at 412 nm of 36,000 M^{-1} cm^{-1}.

High-throughput microtiter plate kinetics

Fibrillation kinetics was measured as previously described (15). Briefly, a fresh glucagon stock solution was made by dissolving powder in 10 mM HCl at a concentration of ~10 g/l; visual clumps were dissolved by gentle pipetting. This stock was diluted to 0.5 g/l glucagon in the appropriate buffer/salts, and transferred to 384/96-well black polystyrene microtiter plates (Nalge Nunc, Rochester, NY). The plate was immediately sealed using crystal clear sealing tape (Hampton Research, Aliso Viejo, CA) to prevent evaporation of samples, and placed in a SpectraMax Gemini XS fluorescence plate reader (Molecular Devices, Sunnyvale, CA). The plate reader was programmed to read fluorescence at 330 and 355 nm ($\lambda_{excitation}$ = 295 nm) and at 502 nm ($\lambda_{excitation}$ = 442 nm) at fixed intervals preceded by a given period of automixing before every read. Noise-reduced fluorescence readings (generally, $F = Em_{355} - 0.48 \times Em_{330}$ was used at acidic pH and $F = Em_{355} - 0.75 \times Em_{330}$ at pH 9.1, where Em_{355} and Em_{330} are the fluorescence intensities observed at 355 and 330 nm, respectively) from every single well were fitted to the following equation using our JSPK software (15):

$$F = (a_m + b_m t) + \frac{(a_f + b_f t)}{\left(1 + ve^{-k(t-t_m)}\right)^{1/v}}, \quad (1)$$

where F is the noise-reduced signal, $a_x + b_x\ t$ are linear equations describing the lag-phase (m) and the equilibrium (f) baselines, t_m is the point of maximum elongation rate, and v describes the asymmetry of the sigmoid curve. The elongation rate is given by $k/(1 + v)$ and the lag-time is defined as $t_m - (1 + v)/k$, which is the time where the tangent at t_m crosses the lag-phase baseline. The apparent nucleation rate is defined as 1/lag time. All fibrillation kinetic data shown in any single figure always originates from a single plate and a single glucagon master stock solution.

We have not verified that the blue shift in Trp emission is always due to fibril formation, under all conditions tested. However, we invariably see a lag phase and an increase in ThT emission concurrently with the Trp blue shift, suggesting that the blue shift is caused by fibril formation. In principle, it should be possible to validate fibril formation by techniques such as size-exclusion chromatography. However, gel filtration is unfeasible as fibrillar glucagon sticks to the column and is eluted in a trailing peak, making it impossible to distinguish from monomeric glucagon (data not shown).

Fluorescence microscopy imaging

Fibrillated samples were transferred directly from microtiter plates to standard microscopy slides, and photographed using a 10× DMR fluorescence microscope (Leica Microsystems, Wetzlar, Germany) with an attached DC200 camera using the I3/FTIC filter cube (excitation BP 450–490 nm, emission dichromatic mirror RKP 510 nm and suppression filter LP 515 nm). Objective magnification of 40× was used.

Electron microscopy

Electron microscopy was carried out as described (20). Briefly, a 5-μl aliquot was placed on a 400-mesh carbon-coated, glow-discharged grid for 30 s. Grids were washed in two drops of double-distilled water and stained with 1% phosphotungstic acid (pH 6.8) and blotted dry on filter paper. Samples were viewed with a Jeol 1010 transmission electron microscope.

Circular dichroism spectra

Fibril samples were sonicated briefly by rod sonication and transferred to a 0.02-cm 106-QS cell (Hellma, Muellheim/Baden, Germany) in a Jasco circular dichroic (CD) spectrometer (Tokyo, Japan) at 25°C. Each reported spectrum is the average of at least three wavelength scans at a speed of 50 nm/min, a band width of 1 nm, and a response time of 2 s. Buffer spectra were subtracted from all reported spectra. All reported [θ] are per-residue values.

ATR-FTIR spectrum

Fibrils were spun down using 10 min centrifugation at 13,000 rpm, and most supernatant was removed. The pellet was transferred to the Germanium crystal at 35°C and dried using a flow of dry N2 gas. The spectra were recorded on an IFS 66v/S Fourier transform infrared (FTIR) spectrometer (Bruker, Ettlingen, Germany). The reported spectra are the average of 32 attenuated total reflection (ATR)-FTIR scans at a resolution of 2 cm^{-1} measured from 4000 to 800 cm^{-1}. Signals from water vapor were removed by subtraction of vapor spectrum. Factor analysis was carried out using Solver in Microsoft Excel.

CD thermostability measurements

Unless otherwise indicated, samples were diluted to 0.05 g/l glucagon in 10 mM HCl with appropriate amounts of salts added in a 4-mm Hellma

119.004F-QS cell. Ellipticity was measured every 0.1°C during temperature ramping at a constant speed of 60°C/h with constant stirring at 540 rpm on a Jasco J-810. Integration time of 2 s and a 2-nm band width were used to reduce signal noise. Raw ellipticity data were fitted to the following equation (37):

$$Y_{obs} = \frac{\alpha_N + \beta_N T + (\alpha_U + \beta_U T)^* e^{-(\frac{\Delta H_{vh}}{R}(\frac{1}{T} - \frac{1}{T_m}))}}{1 + e^{-(\frac{\Delta H_{vh}}{R}(\frac{1}{T} - \frac{1}{T_m}))}}, \quad (2)$$

where Y_{obs} is the observed signal, $(\alpha_x + \beta_x T)$ describes the linear baselines, ΔH_{vh} is the van't Hoff enthalpy change and T_m is the temperature where $\Delta G = 0$. Ellipticity at 235 nm was used to avoid potential contributions from the anomalous readings, which are frequently observed at lower wavelengths (36).

RESULTS

Sulfate is ~65-fold more potent at promoting fibrillation than chloride

We have previously shown, using a combination of Trp and ThT fluorescence, that glucagon can form different types of fibrils at acidic pH, depending on the solvent conditions, such as temperature, glucagon concentration, and the concentration of guanidinium chloride (GdmCl) salt (15). To further investigate the effects of salts on fibrillation, we collected both Trp and in situ ThT fluorescence readings over time at a fixed glucagon concentration (0.5 g/l) and temperature (25°C) in the presence of increasing concentrations of various salts. To minimize contributions from buffer molecules, we decided to adjust pH simply by adding 5 mM HCl which results in a pH of ~2.3. For all concentrations of salts tested, the fibrillation of glucagon resulted in a remarkable blue shift of the Trp fluorescence, which was clearly visible even with the marked quenching at high concentration of, e.g., Cu(II), iodide, and nitrate salts (data not shown). An example of the observed fluorescence time course at different concentrations of NaCl is shown in Fig. 1 *A*. As previously observed, the ThT staining of glucagon fibrils depends on the conditions used for fibrillation (15). In contrast to the Trp fluorescence, which indicates an almost complete depletion of monomeric glucagon, the ThT fluorescence varies with the salt concentration; the increase in ThT intensity relative to starting level varies from 2- to 233-fold, with the highest increases seen for >0.7 mM SO_4^{2-} salts, >10 mM I^-/NO_3^-, and >30 mM Cl^- (Fig. 1 *B*, *top*). In some cases, the ThT intensity even continues to increase, although the plateau formed by the Trp fluorescence signal indicates that monomeric glucagon has been depleted (Fig. 1 *A*; note the logarithmic ThT fluorescence axis). We therefore relied on the Trp fluorescence for quantification of fibrillation kinetics as apparent lag times and elongation rates (Fig. 1 *B*). It is clear that increasing salt concentrations leads to a general increase in the overall fibrillation rates; however, the salts clearly fall into two major groups. To compare the relative potency of the various anions we define a relative potency factor (ρ_x) for each anion:

$$A \equiv \sum \rho_X [X], \quad (3)$$

where A is the apparent potency and $[X]$ is the concentration of anion. If the ρ_x of Cl^- is set to 1, I^- and NO_3^- are set to 1.5, and SO_4^{2-} is set to 65, the fibrillation kinetics and ThT staining/intensity of the resulting fibrils formed (Fig. 1 *B*, *top*) for the all salts are practically superimposed (Fig. 1 *C*). This indicates that the nature of the cation is relatively unimportant and that SO_4^{2-} is ~65-fold more potent than the Cl^- at promoting fibrillation. This effect cannot simply be attributed to a difference in the ionic strength, as 1 mM Na_2SO_4 and $MgSO_4$ only have two- and fourfold greater ionic strength, respectively, than 1 mM NaCl.

For most monovalent anions, there is a small but reproducible bulge on both the apparent lag-time and elongation rates (Fig. 1 *B*), which can be seen around ~16–31 mM, coinciding with the changes in ThT emission intensity (the same decrease is seen for sulfate salts below 0.39 mM). Such drastic changes in ThT staining and fibrillation kinetics often result from changes in the structure of fibrils formed (15). A plot of the apparent lag times versus elongation rates (Fig. S2, Supplementary Material) also shows a high degree of scattering, suggesting that the mechanism by which the fibrils are formed changes with salt concentration. This high degree of scattering could, however, also indicate that the apparent nucleation and elongation rates are affected differently by the salts (19).

Presence of fibrils in the samples containing 1 mM Na_2SO_4 was verified using electron microscopy (Fig. 1 *D*); some of the fibrils formed show regular twisting periods of ~190 nm and individual filaments generally have a width of ~6 nm.

Effects of salts follow the electroselectivity series, not the Hofmeister series

Since only the anion had significant influence on fibrillation kinetics of glucagon at pH 2.3, we further tested other anions, this time at pH 2.0 in 10 mM HCl. As shown in Fig. 2 *A*, thiosulfate has an even stronger effect than sulfate. Anions such as ClO_4^-, which is expected to have a powerful salting-out effect at acidic pH (19), are weak in comparison with SO_4^{2-}, but still lead to significantly shorter lag times than Cl^-. At pH 2.0, the transition from high to low ThT emission is shifted from 16–31 mM (seen at pH 2.3) down to <10 mM for the monovalent anions, with the only exception being $H_2PO_4^-$. The effect of the $H_2PO_4^-$ on fibrillation kinetics is also different from that of other monovalent anions, which may be due to its buffering capacity at pH 2.0 ($pK_a = 2.12$) leading to an increase in pH of the solution with increasing concentration. Indeed, the pH was increased to 3–4 at the highest phosphate concentrations, which apparently results in formation of low-ThT fluorescent type(s) of fibrils. However, at the lowest phosphate concentration (3.9 mM) no fibrils were formed during the incubation, in contrast to a weak fibril formation in 3.9 mM NaCl, indicating that $H_2PO_4^-$ (or the protonated form, H_3PO_4) may be less potent

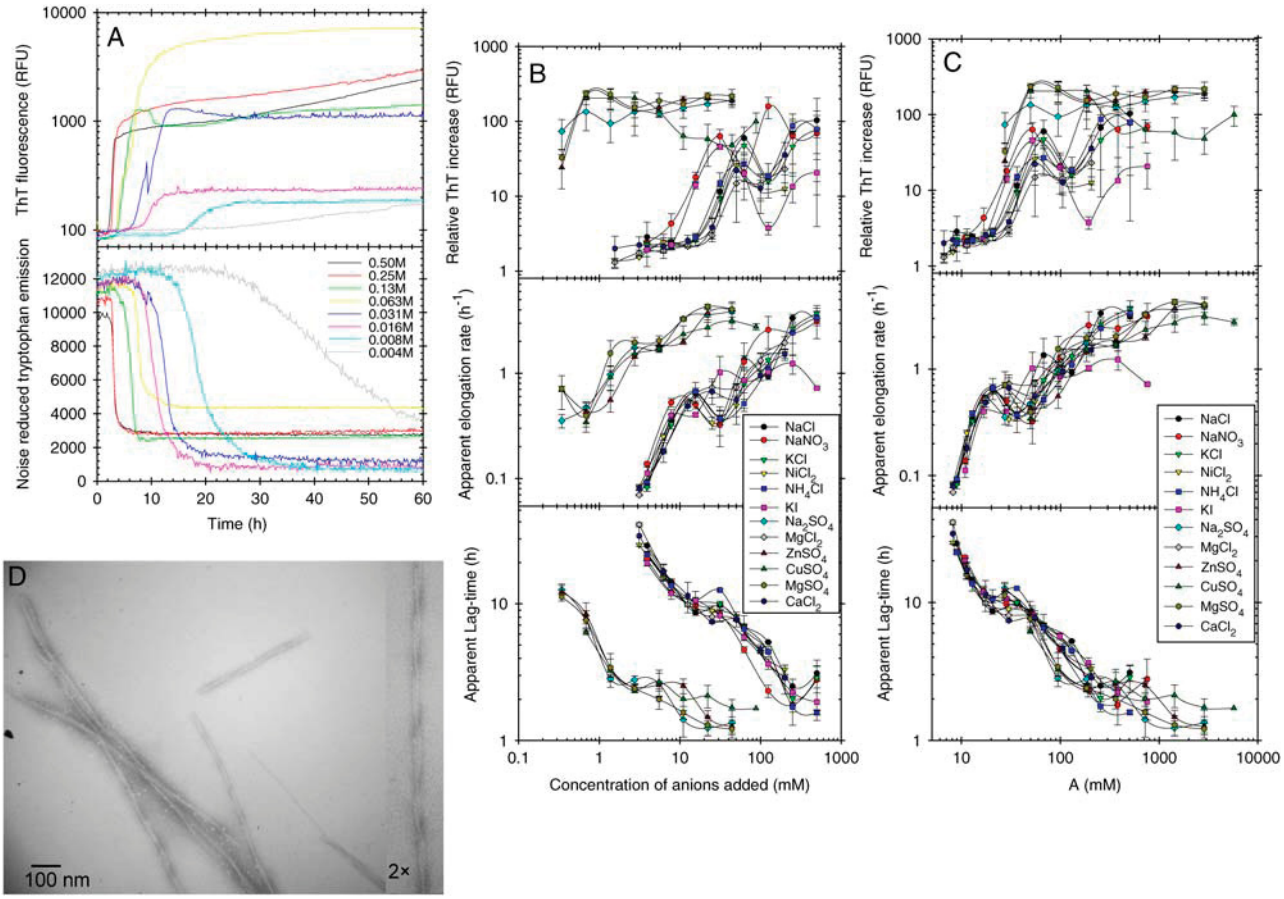

FIGURE 1 Effect of various salts on the fibrillation kinetics of 0.5 g/l glucagon in 5 mM HCl, pH 2.3, with 10 μM ThT (3 s of auto-mixing every 10 min). (*A*) Representative fluorescence observed in single wells with different concentrations of NaCl. (*B*) Kinetic values obtained from fitting noise reduced Trp emission data to Eq. 1 and relative ThT emission intensity increase (end intensity divided by starting intensity) plotted against concentration of anions added (not counting the 5 mM HCl). Error bars indicate the standard deviation of values observed/calculated for three to four replicate wells. (*C*) Same values as in *B*, but plotted against the apparent potency (see text, Eq. 3, and Table 1 for details). (*D*) Electron microscopy image of glucagon fibrils formed in 10 mM HCl with 1 mM Na_2SO_4.

than Cl^- (for a comparison of equilibrium fluorescence wavescans, see Fig. S8). The pH (measured after the assay) was also shifted slightly at the highest concentrations of $Na_2S_2O_3$, but this did not result in changed ThT staining of the fibrils formed (Fig. 2 *A*). This increase in pH indicates that some of the $S_2O_3^{2-}$ anions ($pK_a = 1.72$) are decomposed into HSO_3^- ($S_2O_3^{2-} + H^+ \longleftrightarrow HSO_3^- + S$, $pK_a = 7.2$ (38)) during the assay. In addition, some of the I^- anions were clearly decomposed to free I_2 during the assay, resulting in a brown color. Whether the decay of these anions had any influence on fibrillation kinetics is unknown; however the majority of the ions are expected to have remained intact during the initial critical part of the assay.

A plot of the logarithm of the lag time versus the logarithm of the total Cl^- concentration fits well to a linear equation ($R^2 = 0.96$); using the square root of the concentration instead of the logarithm, appropriate for phenomena involving Debye-Hückel screening, does not lead to a better fit. This simple relationship allows us to quantify the ρ_x (Eq. 3) for other salts using a simple least-squares minimization at intermediate salt concentrations (Fig. S1), giving the values shown in Table 1. The ρ_x of 65–69 for SO_4^{2-} corresponds remarkably well with the factor of 67 (the effect of 3 mM sulfate corresponding to 200 mM chloride) seen for β_2M (18).

Interestingly, the ThT emission intensity is also affected directly by $NaClO_4$, Na_2SO_4, and $Na_2S_2O_3$, increasing exponentially with salt concentrations. This ThT fluorescence, which has a slightly red-shifted emission maximum ($\lambda_{max} = 520$ nm), is caused by the salts, inasmuch as the same increase is also observed without addition of glucagon (Fig. S1). Though there is no clear relationship between the magnitude of the ThT exponential factor and the ρ_x, the relative order of the salts is similar, indicating that the effects may share a common origin (Table 1).

The order of these anions clearly differs from the reverse Hofmeister series observed for fibrillation of α-synuclein (19) ($Cl^- < Br^- \approx H_2PO_4^- < NO_3^- < SO_4^{2-} < S_2O_3^{2-} < ClO_4^-$). This indicates that the effects of the salts on

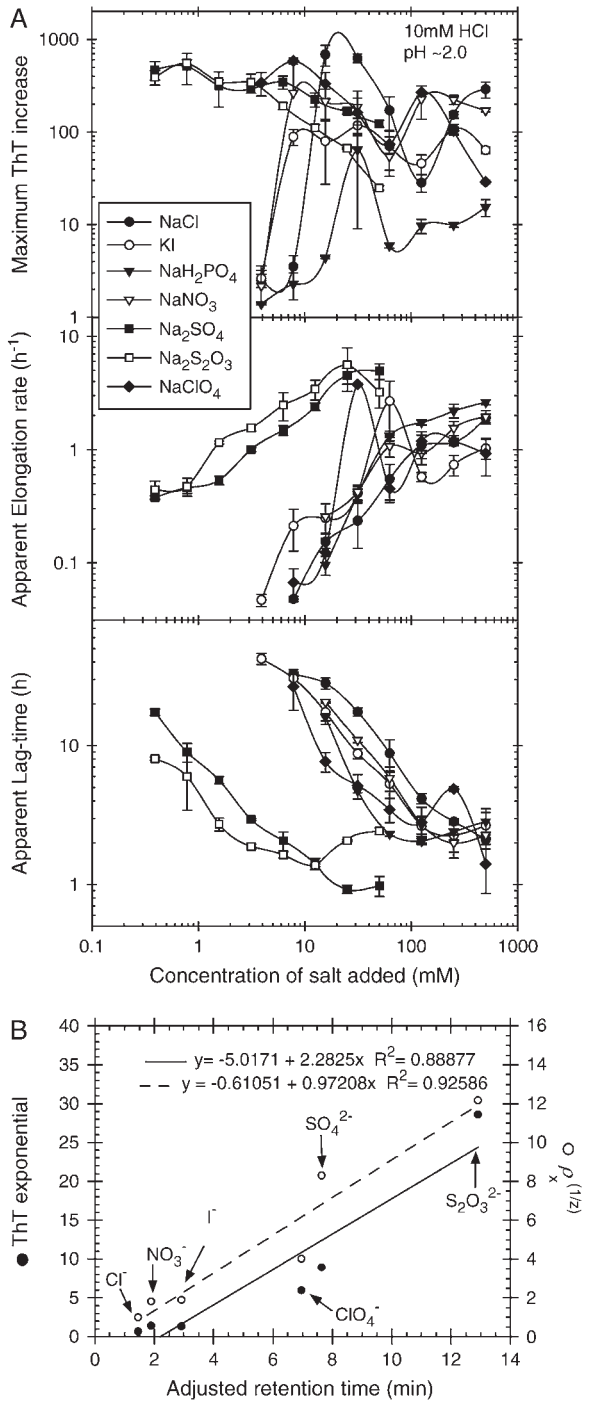

FIGURE 2 (*A*) Effect of various anions on the fibrillation kinetics of 0.5 g/l glucagon with 40 μM ThT in 10 mM HCl, pH 2 (plate read every 10 min with 1 s of auto-mixing between reads). Results are plotted against the concentration of anions added, not counting the 10 mM Cl^- from the 10 mM HCl. Error bars indicate the standard deviation values calculated/observed for three replicate wells. For practical reasons KI was used instead of NaI, however as the cations had a very limited effect this is not expected to significantly affect the results. The ''windows'' with very fast apparent elongation rates, observed at 31 mM $NaClO_4$ and 64 mM KI at pH 2, were also observed in a replicate assay without addition of ThT. (*B*) Plot of numbers shown in Table 1, where the ρ_xs are charge-normalized (z is the charge of the anion).

TABLE 1 Effects of different salts on glucagon fibrillation kinetics

Anion	ρ_x pH 2.3	ρ_x pH 2.0*	ThT exponential†	ρ_x for fibrillation of β_2M‡	Adjusted retention time (min)§
Cl^-	1.0	1.0	0.67	1	1.46
NO_3^-	1.5	1.8	1.43		1.90
I^-	1.5	1.9	1.36	4	2.92
$H_2PO_4^-$		2.0¶	1.71		1.40
ClO_4^-		4.0	6.01	8	6.96
SO_4^{2-}	65	68.8	8.92	67	7.64
$S_2O_3^{2-}$		148.5¶	28.61		12.9

*ρ_x is the relative potency factor for various salts on glucagon fibrillation based on fitting to the double logarithmic correlation between the NaCl concentration and the lag time (Fig. 2 *A*) or from manual fitting of the data in Fig. 1 *B*.

†ThT exponential is the direct effect of salts on ThT emission taken from Fig. 2 *B*.

‡Adapted from Raman et al. (18).

§Adjusted retention times of anions on XAD-1 resin, 0.007 mEq/g with phthalate (1.0×10^{-4} M, pH 6.25) according to Gjerde et al. (40).

¶Due to buffering by these salts, the solution could not be kept at pH 2.0, which may result in overevaluation of the ρ_x.

glucagon fibrillation are not caused by perturbations of the hydrogen-bonding structure of water (39). Instead, the effect of the anions clearly follows the electroselectivity series, which orders the salts according to their retention times on an anion-exchange column (40,41):

$$\begin{aligned} F\text{-} < CH_3COO^- < HCOO^- < H_2PO_4^- < HCO_3^- < Cl^- \\ < NO_2^- < Br^- < NO_3^- < I^- < SCN^- < ClO_4^- < SO_4^{2-} \\ < SO_3^{2-} < C_2O_4^{2-} < CrO_4^{2-} < S_2O_3^{2-}. \end{aligned}$$

(Here we have excluded phosphate because its pK_a of 2.15 affects the pH of the solution and thus the fibrillation kinetics). Generally divalent anions have higher position in the electroselectivity series than monovalent ones due to their higher charge. Anions of equal valency are ordered in the inverse Hofmeister series; because chaotropic anions (like ClO_4^-) interact less favorably with water than kosmotropic ones (like acetate), they bind with higher affinity to the positive resin, yielding greater electroselectivity (42). Effects that follow the electroselectivity series are a clear indication of direct electrostatic interactions between positive charges on protein and negative anions (43). A similar order of salt effects is seen for the fibrillation of β_2-microglobulin at acidic pH (18), from which we have included rough estimates of ρ_x in Table 1 for comparison.

A plot of the charge-normalized potency ($\rho_x^{(1/z)}$) and the ThT fluorescence exponential against the retention time on an anion-exchange column (40) shows a relatively good correlation (Fig. 2 *B*). The fact that charge normalization is required for a good fit could suggest that the glucagon fibrils can either use one divalent anion or two monovalent anions to coordinate the positive charges.

Fluorescence microscopy reveals that high salt concentrations lead to flocculation of fibrils

To investigate whether the salts had any effect on the overall distribution of fibrils in the wells, some of the samples fibrillated at pH 2.0 were viewed in a fluorescence microscope (Fig. S10). Clearly, increased salt concentrations lead to a flocculation of fibrils; despite a fourfold more intense ThT emission in the plate reader at 3.9 mM $NaClO_4$ (Fig. 2 *A*), the fibrils formed were barely visible as very thin threads suspended in the solution (this was difficult to capture photographically). In contrast, larger immobile fibril bundles are clearly visible at 62.5 mM. The same phenomenon was also observed, but at much lowered concentrations, for Na_2SO_4, where fibrils formed at 0.39 mM existed both as bundles and as thin suspended fibers, whereas those formed at 6.25 mM appeared as large ''sponge-like'' clumps.

Cations, not anions, are important at alkaline conditions

Glucagon is capable of fibrillating under alkaline conditions (36), which can be also monitored using both Trp and ThT fluorescence (Fig. S5). We have measured the effect of different anions on the fibrillation of 0.5 g/l glucagon at pH 9.1 (Fig. 3 *A*). At this pH, the lag time also decreases with increasing salt concentration; however, the apparent elongation rate increases only up to 30–50 mM cation regardless of the nature of the anion; at higher concentrations, there is a drop in the apparent elongation rates and a higher ThT fluorescence intensity from the formed fibrils. The apparent fibrillation kinetics and equilibrium ThT staining/fluorescence of fibrils formed are virtually superimposable if plotted against the concentration of the cation (effects of K^+ and Na^+ ions are apparently very similar), but show a higher degree of scattering if plotted against the concentration of the anions. Thus, in contrast to the high potency of divalent anions observed at low pH, the effect of these anions is very limited at pH 9.1. In addition, we have observed that divalent cations, such as Zn^{2+}, play an important role at this slightly alkaline pH. However, because Zn^{2+} also perturbs the Trp fluorescence spectrum of freshly dissolved glucagon, possibly due to trimer formation (44), we have not further investigated the effects of cations at this pH.

Phase diagrams reveal that the fibrillation mechanism is perturbed by the salts

The fluorescence data from Trp and ThT can be combined to investigate the fibrillation mechanism of glucagon (15). When plotting the observed ThT fluorescence against the Trp fluorescence for each time point, there is a clear linear correlation at low salt concentrations. This is seen for 0.39 mM Na_2SO_4 + 10 mM HCl ($R^2 > 0.998$) (Fig. 4 *A*) and 3.9 mM NaCl + 5 mM HCl ($R^2 > 0.98$) (Fig. 4 *B*), but also for

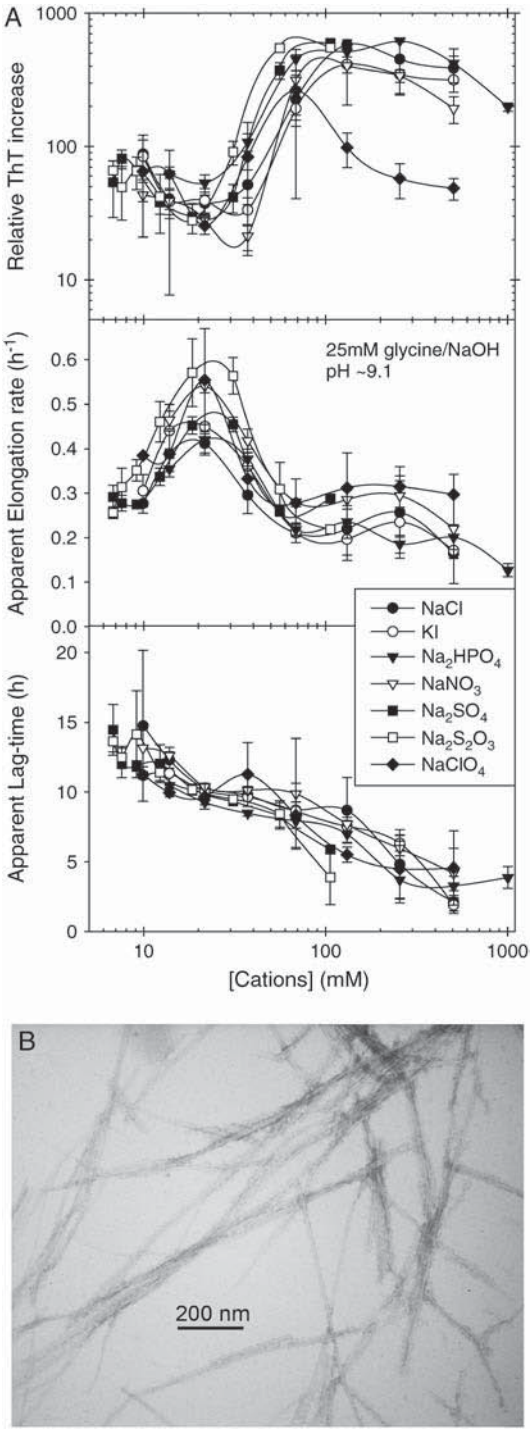

FIGURE 3 (*A*) Effect of various salts on the fibrillation of 0.5 g/l glucagon in 25 mM glycine/NaOH, pH 9.1, with 40 μM ThT (plate read every 10 min with 1 s of auto-mixing between reads). The values are plotted against the concentrations of cations (Na^+ and K^+), including the ~6 mM Na^+ from the buffer. Error bars represent the standard deviation of the values obtained from three replicate wells. (*B*) EM image of fibrils formed at pH 9.5.

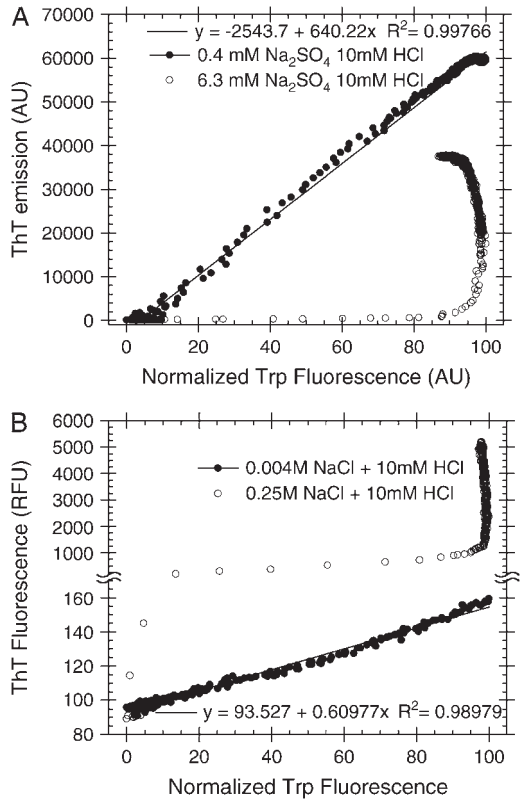

FIGURE 4 Phase diagrams showing the ThT fluorescence versus the normalized Trp emission; a value of 0 indicates lowest, whereas a value of 100 indicates the highest Trp emission intensity change compared to freshly dissolved glucagon. (*A*) Fibrillation of 0.5 g/l glucagon in 10 mM HCl with 40 μM ThT and different concentrations of Na_2SO_4. (*B*) Fibrillation of 0.5 g/l glucagon in 5 mM HCl with 10 μM ThT and different concentrations of NaCl.

other salts. Linearity on such parametric dependence plots or ''phase diagrams'' is a strong indication that intermediate states do not accumulate at significant quantities during fibrillation (45). That is, if any intermediate species do exist, they would have to have exactly the same spectroscopic properties as either the monomeric state or the fibrillar state, which is highly unlikely (15). In contrast, at high salt concentrations, the depletion of monomeric glucagon molecules is generally associated with only a small increase in the ThT fluorescence. After this main transition there is a significant but rather slow increase, long after all monomers are depleted. This indicates that the rapidly formed aggregates; whether they be amorphous aggregates, oligomers, protofibrils, or fibrils, are slowly converted to more ThT stainable and stable structures at high salt concentrations.

There are four possible scenarios that can result in the observed nonlinear phase diagrams:

1. The high salt concentrations simply precipitate glucagons, leading to a slow formation of fibrils.
2. Salts catalyze the nucleation of new fibrils leading to formation of a multitude of nuclei, resulting in a fibril population that consists of many small fibril fragments. Joining together of these small fragments of amyloid (e.g., by end-to-end associations), could produce more ThT binding sites, leading to the gradual increase observed. Fibril assembly from preformed fragments has been observed in an AFM study of insulin fibrillation (46).
3. High salt concentrations lead to rapid formation of individual protofilaments that are slowly joined together in bundles to form mature fibrils, thereby creating more ThT binding sites.
4. More than one type of fibril is formed; the most rapidly formed, low-ThT-stainable fibrils (e.g., type B or D (15)) can be considered an off-pathway intermediate before formation of a more stable ThT-stainable fibril type occurs.

Scenario 1 can be ruled out, because it would require that the amorphous glucagon aggregates give highly blue-shifted Trp emission and that the aggregation process have a lag phase. However, we cannot distinguish between scenarios 2–4 based on the data reported here. Extensive morphological studies would be required for this. From electron microscopy images we have observed that high salt concentrations lead to formation of many short fibrils (data not shown), supporting scenario 2, but this does not rule out the other scenarios.

It should be stressed that all lag times and elongation rates presented in this work result from fitting Eq. 1 to the major transition observed in Trp emission data, which represents depletion of monomeric glucagon (see Materials and Methods) and ignores subsequent gradual transitions.

Sulfate stabilizes α-helical oligomers and leads to formation of fibrils with α-helix-like ''fingerprint'' CD spectrum

The CD spectrum of fibrils formed by 0.5 g/l glucagon in 10 mM HCl + 1 mM Na_2SO_4 looks strikingly similar to CD spectra of proteins rich in α-helices (Fig. 5 *A*), but appears somewhat red-shifted, with a minimum at 225 nm. This is somewhat surprising, since fibrils are generally rich in beta sheet structure (35). However CD spectra are not always easy to interpret as the spectra of β-sheet rich proteins often deviate from the canonical appearance; this is especially so for small peptides rich in aromatic residues (47), glucagon fibrils (15) and proteins rich in Poly(L-Proline)-II (P_2) helices (48).

At somewhat higher sulfate concentrations (50 mM), nonfibrillated (freshly dissolved) glucagon can also adopt a structure with an α-helix-like CD spectrum. However, in comparison with the spectrum of fibrils, the magnitude of the near-ultraviolet (UV) peak for freshly dissolved glucagon is much lower (Fig. 5 *A*, *inset*). Consistent with this lack of near-UV optical activity, we do not observe any significant blue shift in the Trp emission of freshly dissolved glucagon, even at the highest sulfate concentrations (Fig. S6B), indicating that the Trp residue is not perturbed significantly by the increase in α-helical structure.

Formation of secondary structure by freshly dissolved glucagon in the presence of sulfate depends on peptide

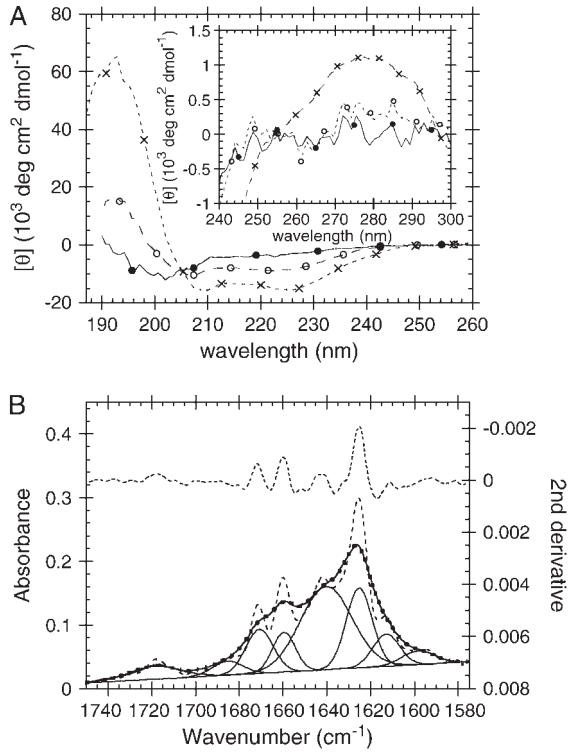

FIGURE 5 (*A*) CD spectra of fresh and fibrillated glucagon in 10 mM HCl: 0.5 g/l (144 μM) freshly dissolved glucagon in 10 mM HCl (●); 1.0 g/l freshly dissolved glucagon in 10 mM HCl with 50 mM Na_2SO_4 (○). Fibrils formed by 0.5 g/l glucagon in 10 mM HCl + 1 mM Na_2SO_4 at 25°C shaking 960 rpm overnight (×). (*Inset*) Near-UV CD of the same samples. (*B*) ATR-FTIR spectrum of fibrils formed by 0.5 g/l glucagon in 10 mM HCl with 1 mM Na_2SO_4. The top curve is the second-derivative, observed spectrum, and Gaussian fits are given by solid lines, sum of Gaussians by a thick dotted line, and Fourier self-deconvoluted spectrum by a dashed line.

concentration (Fig. S6A), indicating that sulfate induces oligomerization, possibly trimerization, as also seen at alkaline conditions (49). NaCl also stabilizes an α-helical conformation of glucagon at pH 2.0, albeit at much higher concentrations (50).

The α-helix stabilization by sulfate and the unusually α-helix-like appearance of the CD spectrum of fibrils could suggest that the fibrils contain large amounts of α-helical structure. However, the ATR FTIR spectrum clearly indicates that the structure of the sulfate induced fibril is mostly β-sheet (Fig. 5 *B*). The small peak at 1660 cm^{-1} could indicate the presence of a small amount of α-helix, but the larger peaks at 1640 and 1625 cm^{-1} are probably caused by (intra- and/or intermolecular) β-sheets (51,52). P_2-helices are expected to have C=O stretching FTIR amide band I peaks in the same region as β-sheets (53).

Sulfate-type fibrils are stabilized by ~22°C for every 10-fold increase in salt concentration

We have previously shown that the stability of glucagon fibrils formed at low pH can be estimated for comparative purposes by thermal scanning CD (15): When the temperature is gradually increased, the CD and Trp-emission spectrum changes cooperatively from that typical for fibrils to that typical for the monomeric peptide, indicating that the fibrils dissociate or ''melt'' into their monomeric components. For the sulfate-type fibrils formed by 0.5 g/l glucagon in the presence of 1 mM sulfate, the ellipticity at 235 nm gives reproducible measurements of apparent thermal melting midpoints (T_m^{app}) (Fig. 6 *A*), despite the unusual appearance of the CD spectrum. For glucagon fibrils formed in 50 mM glycine/HCl, pH 2.5, T_m^{app} is highly dependent on fibrillation temperature (15). However, the T_m^{app} for the sulfate-type fibrils formed in 10 mM HCl and 1 mM Na_2SO_4 is independent of fibrillation temperatures between 25 and 50°C (Fig. S9). Instead, T_m^{app} increases linearly with the logarithm of the concentration of salt added (data not shown). Strikingly, sulfate is two orders of magnitude more stabilizing per mole than chloride, with 5.5 mM sulfate and 500 mM chloride/perchlorate resulting in approximately the same T_m^{app} of ~79°C. In accordance with this, the T_m^{app} of melting at 0.1 mM Na_2SO_4 is higher than expected from the linear correlation because the Cl^- from the 10 mM HCl starts to affect the stability of the fibrils at this very low SO_4^{2-}

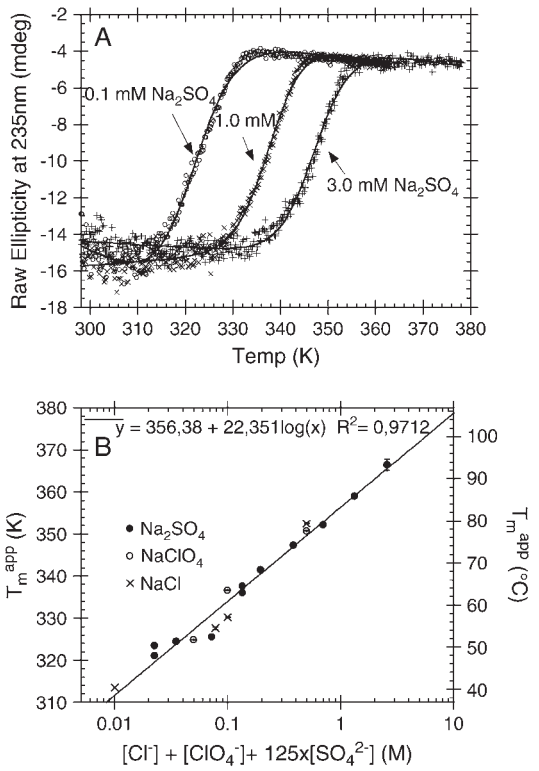

FIGURE 6 Thermal melting of fibrils formed by 0.5 g/l glucagon in 10 mM HCl + 1 mM Na_2SO_4 at room temperature. (*A*) Representative CD thermal scans of 0.05 g/l fibrils in 10 mM HCl with 0.1 (○), 1.0 (×), and 3.0 (+) mM Na_2SO_4 at 60°C/h ramping speed, with solid lines indicating fits to Eq. 2. (*B*) Changes in apparent T_m^{app} (calculated from fitting raw CD data to Eq. 2) as a function of the apparent relative potency of anions.

concentration. This is illustrated by setting the SO_4^{2-} as 125-fold more stabilizing than the monovalent anions, which aligns virtually all apparent T_m^{app}s on a single line (Fig. 6 *B*).

Although the sulfate-type fibrils are relatively stable in acid, increasing pH to neutral (pH 7.4) changes the CD spectrum to that typical for monomeric glucagon within a few minutes (data not shown), suggesting that fibrils dissociate rapidly into monomers. Because both I^-, NO_3^-, and $S_2O_3^{2-}$ absorb UV light, we were not able to measure CD thermal scans in the presence of these anions.

Sulfate-type fibrils can be linearly elongated, but do not grow exponentially at low sulfate concentrations

We have previously shown that when 0.5 g/l glucagon is fibrillated in 50 mM glycine/HCl, pH 2.5, the majority of the resulting fibrils (referred to as ''type B'') exhibit low ThT stainability and a β-turn-like CD spectrum (15). These characteristics are in sharp contrast to the sulfate-type fibrils formed in the presence of 1 mM sulfate, which exhibit high ThT staining/fluorescence and an unusual α-helix-like CD spectrum. These differences could reflect real molecular-level structural diversity (e.g., different secondary structure or packing of glucagon molecules in the fibrils), but could also be induced by a tight interaction between fibrils and sulfate or other salts. In an attempt to distinguish between these two possibilities we conducted seeding experiments under conditions normally resulting in type B fibrils (15) (Fig. 7 *A*). At low seeding fractions, the fibrillation proceeds as previously described (15), leading mainly to formation of type B fibrils. However, at higher seed concentrations, significant amounts of the glucagon molecules are used to elongate the sulfate-type seeds leading to a large increase in the ThT fluorescence. This can be seen from the initial slope of both Trp and ThT fluorescence, which is linearly dependent on the seed concentration (Fig. S7). The change in ThT staining is not due to the small concentration of SO_4^{2-} coming from the seeds, since the effect of the residual <10 μM SO_4^{2-} is expected to be less than the effect of the three orders of magnitude higher Cl^- (~24 mM) concentration (see Table 1). The seed elongation rates are also highly dependent on the concentration of free glucagon (data not shown). Perhaps because of this, the slope of the ThT fluorescence actually decreases over time, as the glucagon monomer concentration decreases (see curve for 5 mg/L seeds in Fig. 7 *A*). Thus, under low sulfate conditions the sulfate-type fibrils are only linearly extended, and not amplified exponentially as would be the case if secondary pathways, such as fibril shearing, branching, or heterogeneous nucleation were involved (15,54). This indicates that SO_4^{2-} ions could be involved in heterogeneous nucleation of sulfate-type fibrils, whereas type B fibrils are amplified via internal scissions (15). This is supported by the fact that the fibrillation kinetics of sulfate-type fibrils is not slowed

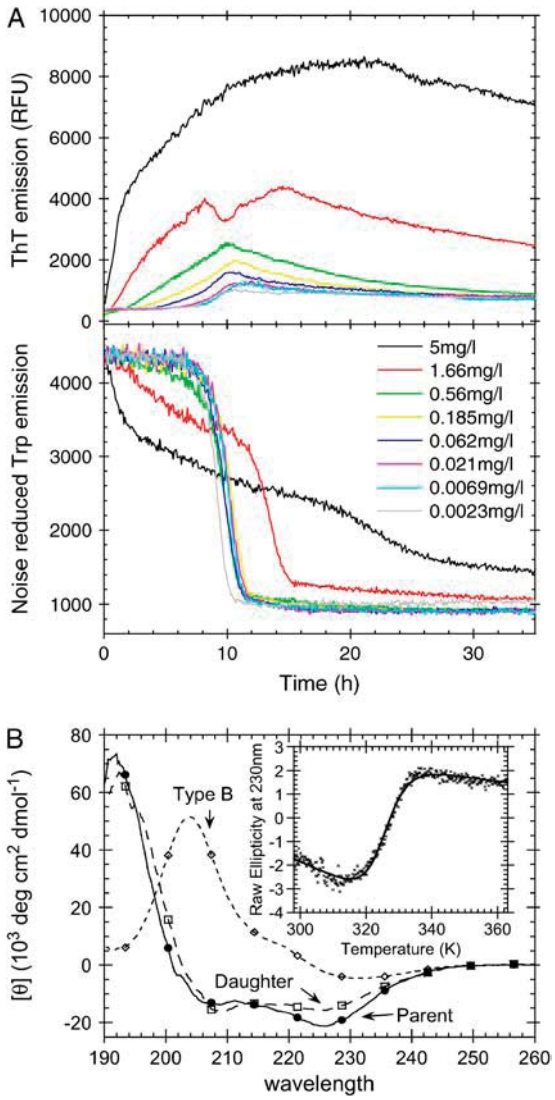

FIGURE 7 (*A*) Fibrillation of 0.5 g/l glucagon in 50 mM glycine/HCl, pH 2.5, with increasing fractions of sonicated fibril seeds (3 s automixing every 5 min). Seeds were formed by 0.5 g/l glucagon in 10 mM HCl + 1 mM Na_2SO_4, pH 2.0. (*B*) CD spectra of fibrils formed by 0.5 g/l glucagon in 50 mM glycine/HCl, pH 2.5 (◇), by 0.5 g/l glucagon in 10 mM HCl + 1mM Na_2SO_4 (parent, ●) and 1g/l glucagon in 50 mM glycine, pH 2.5, with 1% fibrils formed in 10 mM HCl + 1 mM Na_2SO_4 (daughter, □). (*Inset*) Thermal melting of fibrils formed by 0.5 g/l glucagon in 10 mM HCl + 1 mM Na_2SO_4. Melting conditions: 0.025 g/l fibrils in 25 mM glycine, pH 2.7 (0.05 mM residual Na_2SO_4) at 90°C/h ramping speed.

significantly by omitting the automixing between reads (data not shown). Because of the relatively slow elongation of the sulfate-type fibrils, the bulk of the monomeric glucagon has enough time to eventually come together to form type B fibrils. However, as the fibrillation kinetics of type B fibrils is also concentration dependent, the decreased glucagon monomer concentration (due to elongation of seeds) results in a prolonged lag phase for the formation of the type B fibrils at high seed fractions (see the late Trp-fluorescence transition after 20 h in Fig. 7 *A*). Under the conditions of the seeding

assay, type B fibrils have a clear advantage in that they are amplified by secondary pathways (15,54), which result in exponential growth and the sigmoidal curve observed in Fig. 7 *A*. In contrast the sulfate-type fibrils do not appear to be amplified by secondary pathways, and therefore they fail to dominate the resulting fibril population.

We have previously shown that when the glucagon concentration is increased from 0.5 to 1 g/l, the fibrils formed in 50 mM glycine/HCl (consisting of a mixture of type B and type A fibrils) exhibit up to ~21-fold higher ThT intensity per mole glucagon (15). When seeding fibrillation of 1 g/l fresh glucagon with 0.01 g/l sulfate-type fibrils, the seeds are elongated until (nearly) all free glucagon is depleted (as indicated by Trp emission (Fig. S4)), indicating that under these conditions the majority of the fibrils formed are formed by seed elongation. A CD spectrum of these fibrils confirms that the daughter fibrils are indeed of the sulfate type (Fig. 7 *B*).

Interestingly, the apparent stability of sulfate-type fibrils ($T_m^{app} = 52.4 \pm 0.15$°C, Fig. 7 *B*, *inset*) is very similar to that of type B fibrils($T_m^{app} = 52$–55°C (15)). Thus the structure of the fibrils formed does not necessarily correlate with stability, but rather with fibrillation kinetics.

DISCUSSION

Fibril properties can be altered by small changes in pH and salt concentration

Although the change to pH 9.1 clearly changed the effect of the various salts compared to acidic conditions, the smaller change from pH 2.3 (Fig. 1) to 2.0 (Fig. 2) also had a large effect on the type of fibrils formed. At high NaCl concentrations, the fibrillation kinetics are not affected by the small change in pH (compare Fig. 1 *B* and Fig. 2 *A*); however at <32 mM NaCl the fibrils are formed significantly faster at pH 2.3 (lag time <9 h for 21 mM Cl^-) than at pH 2.0 (lag time >25 h for 26 mM Cl^-). In addition, there is a very large (~61-fold) difference in the concentration-normalized equilibrium ThT staining of fibrils formed at 16 mM NaCl upon changing pH from 2.0 to 2.3. We have previously investigated so-called type B glucagon fibrils formed at pH 2.5 under low salt conditions, which are characterized by a low ThT fluorescence and special fingerprint CD spectrum with a positive peak at ~203 nm (15). These type B fibrils are destabilized by decreasing pH, and we therefore suggest that the lowering of pH to 2.3 or 2.0 disfavors the formation of type B fibrils to such an extent that the glucagon molecules have enough time to seek for an alternative, apparently more ThT stainable and acid-resistant ''sulfate type'' of fibril packing. On a molar basis, SO_4^{2-} anions stabilize this type of fibril ~125-fold against thermal melting (Fig. 6) and increase fibrillation rates 65-fold more potently (Table 1) than Cl^- anions. Because of this preferential stabilization, relatively small concentrations of sulfate can trigger formation of the highly ThT-stainable sulfate type of fibrils, even though pH is increased from 2.0 to >2.3, where type B fibrils are stable. It should here also be noted that the sulfate-type fibrils are not stable at neutral pH, similar to fibrils of β_2M formed at acidic pH (55). Since neither sulfate nor chloride ions are deprotonated by changing pH from 2.3 to 7, the observed destabilization of fibrils must be due to deprotonation of acidic residues and/or the carboxy-terminus of the glucagon molecules, resulting in a change from neutral to negative charge. When the pH is increased, the charge repulsion between these negative charges will severely destabilize the fibrils, causing a rapid dissociation, presuming that there are no positive charges to neutralize them. The conversion of negatively charged Asp residues to neutral polar residues at low pH could in theory lead to formation of new favorable side-chain hydrogen bonding (e.g., between two neutral protonated Asp residues), as well as a general increase in fibrillation propensity (56). This could in principle expand the number of possible fibril-packing motifs, as there is a lower absolute number of charged residues (i.e., 5 positive/0 negative = 5 charges at pH 2.5 and 4 positive/4 negative = 8 charges at pH 7), which require either a surface-exposed localization or nearby opposite charges to neutralize them. In addition, all charged residues in glucagon at low pH are located either at the N-terminus (His-1) or in the middle (Lys-12 + Arg-17/18). Nevertheless, all glucagon molecules are positively charged, which is why anions, preferably with high valence, play an important role in the charge screening required for fibril formation.

Preferred fibrillar structure is influenced by the properties of the available anionic ligands

We have previously shown that increasing the glucagon concentration from 0.5 to 1.0 g/l in 50 mM glycine/HCl buffer, pH 2.5, increases the ThT fluorescence of fibrils formed by up to 21-fold per mole of glucagon due to increased formation of highly ThT-fluorescent ''type A'' fibrils instead of low-ThT-stainable type B fibrils formed at low concentrations (15). The changes in fibril staining intensity observed upon adding 1 mM sulfate during fibrillation at pH 2.3 are of an even larger magnitude, with fibrils formed at ~1 mM SO_4^{2-}, leading to a ThT fluorescence increase of ~200-fold in contrast to the ~3-fold increase observed at ~10 mM Cl^- (Fig. 1 *B*). This suggests that sulfate anions may stabilize the same type of fibrils that are formed at high concentrations of glucagon: Although the stability of type B fibrils, which do not seem to depend on buffer molecules, is relatively high ($T_m^{app} \approx 53$°C), the stability of type A fibrils is very low ($T_m^{app} \approx 32$°C, conditions for thermal scan: 0.025 g/l glucagon, 25 mM glycine/HCl, pH 2.7, ramping speed 90°C/h (15)). The latter corresponds well with the T_m^{app} expected (~34°C, Fig. 6 *B*) for a solution containing only 12 mM Cl^- (not considering the differences in assay conditions). The CD and FTIR

spectra and the electron microscopy images show some deviations between the two aggregates. This could be due to both sample heterogeneity and to specific binding of sulfate anions to fibrils, which could lead to fixing of local flexible loops and subsequent spectral changes. We plan to deploy other structural techniques to establish whether these two types of aggregates share the same kind packing motif.

It has previously been shown that intermediate concentrations of Cl^- (~100–500 mM) can result in the formation of type D glucagon fibrils, which are characterized by a clear β-sheet CD signature and low ThT staining (15); higher Cl^- concentrations result in high ThT staining that may well stem from fibrils similar to the sulfate-type fibrils described in this work (see Fig. 8). Although the low-ThT-stainable intermediate formed at high SO_4^{2-} concentrations (cfr. nonlinear phase diagram at 6.3 mM Na_2SO_4 in Fig. 4 *A*) could well be type D fibrils, none of the tested concentrations of SO_4^{2-} resulted in stable formation of type D fibrils. This suggests that the preferred fibrillar structure of a peptide may be dictated by the spatial stereochemistry of anionic ligands available in the solution (i.e., Cl^- ions stabilize type D fibrils and SO_4^{2-} ions drive the formation of sulfate-type fibrils.). Indeed, it has been suggested that the strain-specific conformation of prion-protein fibrils is determined by metal ions (57).

Do the helical oligomers play a role in the fibrillation process?

It has previously been shown that glucagon forms helical trimers at alkaline pH (49). If these α-helical oligomers are stable enough, they could in theory prevent fibrillation of glucagon by depleting monomeric glucagon from the solution. This is seen for proteins with a compact native structure, e.g., β_2M (18), TTR (26), and insulin (17), where fibrillation is slowed down at high salt concentrations due to stabilization of the native conformations/oligomerizations. Salts are known to stabilize the glucagon trimers formed at alkaline conditions (58), which may be the reason why we see the decrease in elongation rates observed at >20–30 mM Na^+ concentrations at pH 9.1. This could indicate that above this salt concentration a significant fraction of the glucagon molecules are engaged in trimerization. However, because the solubility of glucagon around pH 9 is ~2 g/l (depending on ionic strength, data not shown) it is also possible that the increased salt concentration results in phase separation due to precipitation of trimers or amorphous aggregates.

The C-terminal residues of freshly dissolved glucagon are known to be involved in concentration-dependent aggregation at acidic pH (59). In addition, high concentrations of sodium chloride salts stabilize α-helical structure of glucagon, suggesting oligomer formation (50). Our results suggest that the α-helical oligomers formed under acidic conditions are stabilized by relatively low concentrations of sulfate. But in contrast to what is seen under alkaline conditions, the elongation rates seem to increase monotonically with increasing salt concentrations at low pH. Thus, if any oligomers are formed due to high salt concentrations they do not seem to inhibit the fibrillation significantly, possibly because the salts also stabilize fibrils. Our seeding experiments suggest that the elongation proceeds via the addition of monomers rather than oligomers (Fig. 7), analogous to what is seen for prion amyloid (60). However, it cannot be ruled out that the sulfate-dependent oligomers may play

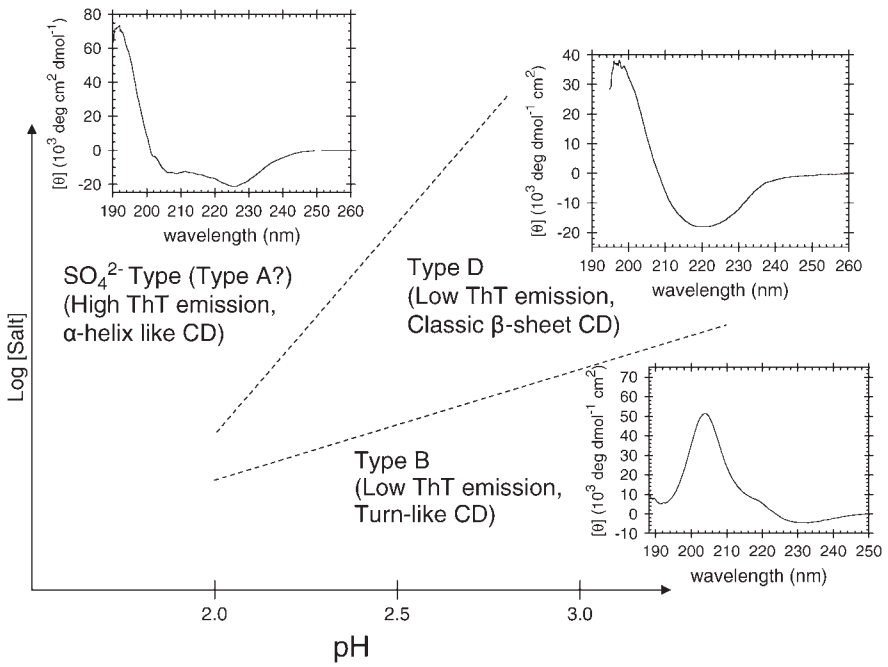

FIGURE 8 Schematic overview over which conditions result in the different types of fibrils glucagon can form at acidic pH. Type A, B, and D fibrils refer to glucagon fibril types previously described (15), whereas sulfate-type refers to the type described in this article.

a role in the secondary pathways of the fibrillation (54), e.g., if the helical sulfate-glucagon complexes are involved in heterogeneous nucleation on the surface of existing fibrils.

Are sulfate anions natural amyloid ligands?

In addition to having strong stabilizing effects at decimolar concentrations, lower concentrations of sulfate ions are also known to stabilize both the molten globule (61) and the native (62) protein structures at acidic pH. This is seen from a 20°C increase in T_m for ribonuclease A at pH 2.0 upon addition of 0.1 M Na_2SO_4 (62). The sulfate-induced stabilization of the sulfate-type glucagon fibrils is even stronger with a 22°C increase in T_m^{app} for every 10-fold increase in SO_4^{2-} concentration (Fig. 6 *B*). Our stability measurements were actually limited by the stability of the fibrils approaching 100°C for only ~50 mM Na_2SO_4, which is below the concentrations at which stabilizing Hofmeister effects are expected to be significant (62). The strong correlation between the effects of the different anions and the position in the electroselectivity series (Fig. 2 *B*) is a clear indication of direct electrostatic interaction between the positively charged fibrils and the negative anions (43), which may act as structural ligands to the fibrils.

Sulfate ions are known to induce a marked lateral association of preformed Aβ-fibrils (25) and also aggregates fibrils formed by TTR (26). Truncation mutagenesis of Aβ and the fact that lateral aggregation was not observed at pH >8 indicates that the protonated His residues are important for the binding of sulfate to Aβ fibrils, whereas Lys residues are not important (25). Despite the low resolution of the fluorescence microscope, it is clear that the glucagon fibrils formed at higher concentrations of salts appear as large clumps compared to the more dispersed fibrils formed at lower salt concentrations (Fig. S10). Therefore the large stabilizing effect of sulfate on the fibrillated form of glucagon could be due to clumping (resulting in low surface/mass ratio) of fibrils as well as stabilizing effects of direct sulfate-ligand binding to fibrils.

The binding of SO_4^{2-} anions to Aβ-peptide-derived fibrils gives rise to an intense 65-Å meridional reflection that presumably arises from the periodic deposition of sulfate along the axis of the fibrils (25). The regularity of this reflection suggests that the interaction is specific, but the distance also suggests there may be more to the fibril structure than just a simple regular stacking of β-strands.

One of the features common to all ex vivo amyloids is the presence of highly sulfated glycosaminoglycans (27,63). Sulfate anions have been shown to compete for the same binding sites as the GAGs on ex vivo inflammation-associated amyloid, with addition of sulfate resulting in increased exposure of amino acid side chains to chemical modification (28). This is a strong indication that the GAGs interact with amyloids through their sulfate moieties, even though covalently bound sulfate groups only have one negative charge. In addition, it has been shown that fibrils of β_2M formed at acidic pH, which would normally dissociate at neutral pH, are stabilized by GAGs so that they can exist at neutral pH (55). The strong stabilization of both glucagon and β_2M fibrils suggests that the shape/size of the sulfate anions is suitable for interaction with (the positive charges on) proteins in an amyloid-like β-sheet conformation. In contrast, the effect of anions (>10 mM) on the fibrillation of α-synuclein appear to be limited to salting-out effects (19). However, α-synuclein is a remarkable natively unstructured protein, which contains 15 Lys residues but not a single Arg and only one His residue, despite having a sequence length of 140 residues (64). This suggests that α-synuclein must be under selective pressure not to have any Arg, since statistically 6 of 64 codons (~9%) should encode Arg. This also suggests that Arg, in addition to His (25), may be important for the interactions between sulfate anions and amyloid. One could further hypothesize that the reason for the lack of Arg residues in α-synuclein is that this natively unfolded protein would otherwise be ''fair game'' to the physiological concentrations of ''amyloid-inducing'' sulfate/GAGs available in the human brain.

SUPPLEMENTARY MATERIAL

An online supplement to this article can be found by visiting BJ Online at http://www.biophysj.org.

Professor Gunna Christiansen is acknowledged for the electron microscopy images.

J.S.P. was supported by a PhD stipend cofinanced by Aalborg University and Novo Nordisk A/S.

REFERENCES

1. Jarrett, J. T., and P. T. Lansbury, Jr. 1993. Seeding ''one-dimensional crystallization'' of amyloid: a pathogenic mechanism in Alzheimer's disease and scrapie? *Cell*. 73:1055–1058.
2. Sunde, M., L. C. Serpell, M. Bartlam, P. E. Fraser, M. B. Pepys, and C. C. Blake. 1997. Common core structure of amyloid fibrils by synchrotron X-ray diffraction. *J. Mol. Biol.* 273:729–739.
3. Geddes, A. J., K. D. Parker, E. D. Atkins, and E. Beighton. 1968. Cross-β" conformation in proteins. *J. Mol. Biol.* 32:343–358.
4. Dobson, C. M. 1999. Protein misfolding, evolution and disease. *Trends Biochem. Sci.* 24:329–332.
5. Kelly, J. W., and W. E. Balch. 2003. Amyloid as a natural product. *J. Cell Biol.* 161:461–462.
6. Anfinsen, C. B. 1973. Principles that govern the folding of protein chains. *Science*. 181:223–230.
7. Fersht, A. R. 1999. Structure and Mechanism in Protein Science. A Guide to Enzyme Catalysis and Protein Folding: W. H. Freeman and Company, New York.
8. Tanaka, M., P. Chien, N. Naber, R. Cooke, and J. S. Weissman. 2004. Conformational variations in an infectious protein determine prion strain differences. *Nature*. 428:323–328.
9. Bauer, H. H., U. Aebi, M. Haner, R. Hermann, M. Muller, and H. P. Merkle. 1995. Architecture and polymorphism of fibrillar supramolecular assemblies produced by in vitro aggregation of human calcitonin. *J. Struct. Biol.* 115:1–15.

10. Goldsbury, C. S., G. J. Cooper, K. N. Goldie, S. A. Muller, E. L. Saafi, W. T. Gruijters, M. P. Misur, A. Engel, U. Aebi, and J. Kistler. 1997. Polymorphic fibrillar assembly of human amylin. *J. Struct. Biol.* 119:17–27.

11. Jimenez, J. L., E. J. Nettleton, M. Bouchard, C. V. Robinson, C. M. Dobson, and H. R. Saibil. 2002. The protofilament structure of insulin amyloid fibrils. *Proc. Natl. Acad. Sci. USA.* 99:9196–9201.

12. Serpell, L. C., M. Sunde, M. D. Benson, G. A. Tennent, M. B. Pepys, and P. E. Fraser. 2000. The protofilament substructure of amyloid fibrils. *J. Mol. Biol.* 300:1033–1039.

13. Petkova, A. T., R. D. Leapman, Z. Guo, W. M. Yau, M. P. Mattson, and R. Tycko. 2005. Self-propagating, molecular-level polymorphism in Alzheimer's beta-amyloid fibrils. *Science.* 307:262–265.

14. Dzwolak, W., V. Smirnovas, R. Jansen, and R. Winter. 2004. Insulin forms amyloid in a strain-dependent manner: an FT-IR spectroscopic study. *Protein Sci.* 13:1927–1932.

15. Pedersen, J. S., D. Dikov, J. L. Flink, H. A. Hjuler, G. Christiansen, and D. E. Otzen. 2006. The changing face of glucagon fibrillation: structural polymorphism and conformational imprinting. *J. Mol. Biol.* 355:501–523.

16. Uversky, V. N., and A. L. Fink. 2004. Conformational constraints for amyloid fibrillation: the importance of being unfolded. *Biochim. Biophys. Acta.* 1698:131–153.

17. Nielsen, L., R. Khurana, A. Coats, S. Frokjaer, J. Brange, S. Vyas, V. N. Uversky, and A. L. Fink. 2001. Effect of environmental factors on the kinetics of insulin fibril formation: elucidation of the molecular mechanism. *Biochemistry.* 40:6036–6046.

18. Raman, B., E. Chatani, M. Kihara, T. Ban, M. Sakai, K. Hasegawa, H. Naiki, M. Rao Ch, and Y. Goto. 2005. Critical balance of electrostatic and hydrophobic interactions is required for beta 2-microglobulin amyloid fibril growth and stability. *Biochemistry.* 44:1288–1299.

19. Munishkina, L. A., J. Henriques, V. N. Uversky, and A. L. Fink. 2004. Role of protein-water interactions and electrostatics in α-synuclein fibril formation. *Biochemistry.* 43:3289–3300.

20. Pedersen, J. S., G. Christensen, and D. E. Otzen. 2004. Modulation of S6 fibrillation by unfolding rates and gatekeeper residues. *J. Mol. Biol.* 341:575–588.

21. Ries-Kautt, M. M., and A. F. Ducruix. 1989. Relative effectiveness of various ions on the solubility and crystal growth of lysozyme. *J. Biol. Chem.* 264:745–748.

22. Timasheff, S. N. 2002. Protein hydration, thermodynamic binding, and preferential hydration. *Biochemistry.* 41:13473–13482.

23. Mantyh, P. W., J. R. Ghilardi, S. Rogers, E. DeMaster, C. J. Allen, E. R. Stimson, and J. E. Maggio. 1993. Aluminum, iron, and zinc ions promote aggregation of physiological concentrations of β-amyloid peptide. *J. Neurochem.* 61:1171–1174.

24. Huang, X., C. S. Atwood, R. D. Moir, M. A. Hartshorn, R. E. Tanzi, and A. I. Bush. 2004. Trace metal contamination initiates the apparent auto-aggregation, amyloidosis, and oligomerization of Alzheimer's Aβ peptides. *J. Biol. Inorg. Chem.* 9:954–960.

25. Fraser, P. E., J. T. Nguyen, D. T. Chin, and D. A. Kirschner. 1992. Effects of sulfate ions on Alzheimer β/A4 peptide assemblies: implications for amyloid fibril-proteoglycan interactions. *J. Neurochem.* 59:1531–1540.

26. Bonifacio, M. J., Y. Sakaki, and M. J. Saraiva. 1996. 'In vitro' amyloid fibril formation from transthyretin: the influence of ions and the amyloidogenicity of TTR variants. *Biochim. Biophys. Acta.* 1316:35–42.

27. Snow, A. D., J. Willmer, and R. Kisilevsky. 1987. Sulfated glycosaminoglycans: a common constituent of all amyloids? *Lab. Invest.* 56:120–123.

28. Wong, S., and R. Kisilevsky. 1990. Influence of sulphate ions on the structure of AA amyloid fibrils. *Scand. J. Immunol.* 32:225–232.

29. Goedert, M., R. Jakes, M. G. Spillantini, M. Hasegawa, M. J. Smith, and R. A. Crowther. 1996. Assembly of microtubule-associated protein tau into Alzheimer-like filaments induced by sulphated glycosaminoglycans. *Nature.* 383:550–553.

30. Perez, M., J. M. Valpuesta, M. Medina, E. Montejo de Garcini, and J. Avila. 1996. Polymerization of τ into filaments in the presence of heparin: the minimal sequence required for τ-τ interaction. *J. Neurochem.* 67:1183–1190.

31. Kampers, T., P. Friedhoff, J. Biernat, E. M. Mandelkow, and E. Mandelkow. 1996. RNA stimulates aggregation of microtubule-associated protein τ into Alzheimer-like paired helical filaments. *FEBS Lett.* 399:344–349.

32. Necula, M., C. N. Chirita, and J. Kuret. 2003. Rapid anionic micelle-mediated α-synuclein fibrillization in vitro. *J. Biol. Chem.* 278:46674–46680.

33. Bromer, W. W., A. Staub, E. R. Diller, H. L. Bird, L. G. Sinn, and O. K. Behrens. 1957. The amino acid sequence of glucagon. *J. Am. Chem. Soc.* 79:2794–2798.

34. Beaven, G. H., W. B. Gratzer, and H. G. Davies. 1969. Formation and structure of gels and fibrils from glucagon. *Eur. J. Biochem.* 11:37–42.

35. Glenner, G. G., E. D. Eanes, H. A. Bladen, R. P. Linke, and J. D. Termine. 1974. β-Pleated sheet fibrils. A comparison of native amyloid with synthetic protein fibrils. *J. Histochem. Cytochem.* 22:1141–1158.

36. Moran, E. C., P. Y. Chou, and G. D. Fasman. 1977. Conformational transitions of glucagon in solution: the α to β transition. *Biochem. Biophys. Res. Commun.* 77:1300–1306.

37. Yadav, S., and F. Ahmad. 2000. A new method for the determination of stability parameters of proteins from their heat-induced denaturation curves. *Anal. Biochem.* 283:207–213.

38. Lide, D. R., editor. 2005. Physical Constants of Organic Compounds, 85th ed. CRC Press, Boca Raton, FL.

39. Baldwin, R. L. 1996. How Hofmeister ion interactions affect protein stability. *Biophys. J.* 71:2056–2063.

40. Gjerde, D. T., G. Schmuckler, and J. S. Fritz. 1980. Anion chromatography with low-conductivity eluents. II. *J. Chromatogr.* 187:35–45.

41. Gregor, H. P., J. Belle, and R. A. Marcus. 1955. Studies on ion-exchange resins. XIII. selectivity coefficients of quaternary Base Anion-exchange Resins Toward Univalent Anions. *J. Am. Chem. Soc.* 77:2713–2719.

42. Menon, M. K., and A. L. Zydney. 1999. Effect of ion binding on protein transport through ultrafiltration membranes. *Biotechnol. Bioeng.* 63:298–307.

43. Goto, Y., N. Takahashi, and A. L. Fink. 1990. Mechanism of acid-induced folding of proteins. *Biochemistry.* 29:3480–3488.

44. Epand, R. M. 1982. Cation-induced conformational change in glucagon. *Mol. Pharmacol.* 22:105–108.

45. Ahmad, A., I. S. Millett, S. Doniach, V. N. Uversky, and A. L. Fink. 2003. Partially folded intermediates in insulin fibrillation. *Biochemistry.* 42:11404–11416.

46. Jansen, R., W. Dzwolak, and R. Winter. 2005. Amyloidogenic self-assembly of insulin aggregates probed by high resolution atomic force microscopy. *Biophys. J.* 88:1344–1353.

47. Colon, W. 1999. Analysis of protein structure by solution optical spectroscopy. *Methods Enzymol.* 309:605–632.

48. Sreerama, N., and R. W. Woody. 2003. Structural composition of βI- and βII-proteins. *Protein Sci.* 12:384–388.

49. Gratzer, W. B., J. M. Creeth, and G. H. Beaven. 1972. Presence of trimers in glucagon solution. *Eur. J. Biochem.* 31:505–509.

50. Wu, C. S., and J. T. Yang. 1980. Helical conformation of glucagon in surfactant solutions. *Biochemistry.* 19:2117–2122.

51. Seshadri, S., R. Khurana, and A. L. Fink. 1999. Fourier transform infrared spectroscopy in analysis of protein deposits. *Methods Enzymol.* 309:559–576.

52. Zandomeneghi, G., M. R. Krebs, M. G. McCammon, and M. Fandrich. 2004. FTIR reveals structural differences between native β-sheet proteins and amyloid fibrils. *Protein Sci.* 13:3314–3321.

53. Swenson, C. A., and R. Formanek. 1967. Infrared study of poly-L-proline in aqueous solution. *J. Phys. Chem.* 71:4073–4077.

54. Ferrone, F. 1999. Analysis of protein aggregation kinetics. *Methods Enzymol.* 309:256–274.

55. Yamaguchi, I., H. Suda, N. Tsuzuike, K. Seto, M. Seki, Y. Yamaguchi, K. Hasegawa, N. Takahashi, S. Yamamoto, F. Gejyo, and H. Naiki. 2003. Glycosaminoglycan and proteoglycan inhibit the depolymerization of β2-microglobulin amyloid fibrils in vitro. *Kidney Int.* 64: 1080–1088.

56. Pawar, A. P., K. F. Dubay, J. Zurdo, F. Chiti, M. Vendruscolo, and C. M. Dobson. 2005. Prediction of ''aggregation-prone'' and ''aggregation-susceptible'' regions in proteins associated with neurodegenerative diseases. *J. Mol. Biol.* 350:379–392.

57. Wadsworth, J. D., A. F. Hill, S. Joiner, G. S. Jackson, A. R. Clarke, and J. Collinge. 1999. Strain-specific prion-protein conformation determined by metal ions. *Nat. Cell Biol.* 1:55–59.

58. Formisano, S., M. L. Johnson, and H. Edelhoch. 1978. Effects of Hofmeister salts on the self-association of glucagon. *Biochemistry.* 17: 1468–1473.

59. Patel, D. J. 1970. Proton nuclear magnetic resonance study of glucagon. *Macromolecules.* 3:448–449.

60. Collins, S. R., A. Douglass, R. D. Vale, and J. S. Weissman. 2004. Mechanism of prion propagation: amyloid growth occurs by monomer addition. *PLoS Biol.* 2:e321.

61. Goto, Y., and S. Nishikiori. 1991. Role of electrostatic repulsion in the acidic molten globule of cytochrome c. *J. Mol. Biol.* 222:679–686.

62. Ramos, C. H., and R. L. Baldwin. 2002. Sulfate anion stabilization of native ribonuclease A both by anion binding and by the Hofmeister effect. *Protein Sci.* 11:1771–1778.

63. Kisilevsky, R., and A. Snow. 1988. The potential significance of sulphated glycosaminoglycans as a common constituent of all amyloids: or, perhaps amyloid is not a misnomer. *Med. Hypotheses.* 26:231–236.

64. Davidson, W. S., A. Jonas, D. F. Clayton, and J. M. George. 1998. Stabilization of α-synuclein secondary structure upon binding to synthetic membranes. *J. Biol. Chem.* 273:9443–9449.